Geophysica (1992), 28, 1-2,15-27

Numerical Modelling of 2-D Electric Conductivity Variations in Earthquake Preparatory Areas

Waldemar Jozwiak[1], *Klaus Meyer*[2] *and Tomasz Ernst*[1]

[1]Institute of Geophysics, Polish Academy of Science, Warsaw, Poland
[2]Seismological Department, Box 2101, S-750 02 Uppsala, Sweden

(Received: November 1992; Accepted: April 1993)

Abstract

The electric conductivity of the crust depends strongly on the state and evolution of microcracks in the vicinity of an earthquake preparational stress system. The electrical resistivity is highly sensitive to stress induced crack development (orientation, rate of growth, opening and closing of cracks) and subsequent threshold processes (crack density, water percolation, electrokinetic phenomena). Temporal changes of resistivity are thus related to stress variations, passing through the preseismic, coseismic and postseismic stages of an earthquake cycle. Resistivity changes in an earthquake preparational area will provide corresponding changes of electromagnetic induction, and will hence produce "anomalous" variations in the electric field. Using a tentative model of temporal resistivity changes in an anticipated elliptic earthquake preparational zone, we compute the apparent resistivity response for some simple cases of resistivity structure. The numerical results show that the ratio of electric vs magnetic field variations (proportional to the square-root of apparent resistivity) may change in time by up to several orders of magnitude, depending on the model considered.

1. Introduction

The electric conductivity of the lithosphere basically depends on the geological structure. Possible time variations of this conductivity may be related to the state and evolution of microcracks in the presence of lithospheric stresses, for instance in the vicinity of an earthquake preparatory stress system. The electric conductivity is highly sensitive to stress induced crack development such as crack orientation, crack density and opening or closing of cracks. In the ultimate stage of an earthquake cycle (imminent rupture) we also expect threshold processes in form of crack nucleation and possibly percolation of water into the system of cracks. Any temporal changes of resistivity due to microcrack evolution will certainly also alter the apparent resistivity and thus the effects of electromagnetic induction, in particular in the imminent stage of a forthcoming earthquake. It is thus of interest to find out whether or not "anomalous" variations in the Earth's telluric field (electric field), ETF, have any relation with tectonophysical source processes prior to earthquake rupture and may thus be considered as earthquake precursors. The existance of

geophysical earthquake forerunners in the ETF has been suggested in numerous investigations. An extensive review has been summarized by *Bernhard* (1992). Even though poorly understood today, ETF precursors are certainly part of the complex geophysical processes in and around the earthquake preparational area. Thus their further investigation will contribute to the qualitative understanding of source processes in the earthquake fault zone.

Measurable changes of the resistivity in seismically active regions have been reported by, for instance, *Barsukov* (1972), *Barsukov* and *Sorokin* (1973), Mazella and *Morrison* (1974), *Niblett* and *Honkura* (1978), *Zadro et al.* (1990) or *Ernst et al.* (1991). They report apparent resistivity changes of up to 24% prior to earthquakes. Continuous rock resistivity measurements in active mines in Poland show that the resistivity can change up to one order of magnitude prior to rockbursts induced by mining activities (*Stopinski* and *Teisseyre*, 1982). *Meyer* and *Teisseyre* (1988, 1989) and *Teisseyre* (1991) explain anomalous ETF variations by time-variable electromagnetic induction, due to resistivity changes related to opening and closing of cracks and water transport between cracks. *Teisseyre* (1983) attempts to explain observed resistivity changes in Polish copper mines prior to rockbursts. In an area of dry dilatancy the resistivity increases slowly until a threshold process is reached, when water starts to percolate into the system of microcracks. At this stage the resistivity decreases drastically.

Following the concept of time-variable apparent resistivity changes in the vininity of an earthquake preparational stress system (microcrack evolution) we attempt to compute the corresponding apparent resistivity response. The quantitative results should provide an impression about the magnitude of possible time variations of apparent resistivities and should thus give us suggestions about the corresponding "anomalous" variations in the ETF.

2. *Apparent resistivity changes*

In the field simultaneous measurements of the magnetic field components H and D and electric recordings of two electric lines, directed N-S and E-W, are carried out. Magnetic components induce electric fields E_{EW} and E_{NS}. The relationship of electromagnetic induction in frequency domain is the following:

$$\begin{bmatrix} E_{NS}(\omega) \\ E_{EW}(\omega) \end{bmatrix} = \begin{bmatrix} Z_{11}(\omega) & Z_{12}(\omega) \\ Z_{21}(\omega) & Z_{22}(\omega) \end{bmatrix} \begin{bmatrix} H(\omega) \\ D(\omega) \end{bmatrix} \tag{1}$$

Z_{ik} is an impedance tensor representing the transfer function between the electric component E_i ($E_1 = E_{NS}$, $E_2 = E_{EW}$) and the magnetic components H_K ($H_1 = H$, $H_2 = D$).

The apparent resistivity $\rho_A(\omega)$ is deduced from the impedance tensor, i.e.

$$\rho_{A,ik}(\omega) = |Z_{ik}(\omega)|^2/\mu\omega \tag{2}$$

where μ is magnetic permeability.

The state of stress governs the evolution of microcracks as mentioned above. This will alter the resistivity in the focal area and subsequently the apparent resistivity measured on the surface. Thus, we expect a time dependence of apparent resistivity

$$\rho_{A,\,ik} = \rho_{A,\,ik}(\omega,t) \tag{3}$$

Below we give an example (cf. *Meyer* and *Teisseyre*, 1988, 1989) of a tentative variation of resistivity in the focal region of a forthcoming earthquake (Fig. 1). A dilatancy in dry or partly saturated rocks leads to a resistivity increase. We may expect the same type of a resistivity increase in saturated rocks if we consider a sector of compression. In that case a kind of "water out-squeezing" effect can be assumed. The start of the resistivity drop (Fig. 1) describes the formation of the fracture plane, i.e. the threshold process of crack evolution (crack nucleation). In this phase water percolation starts a drastic decrease of resistivity (see *Meyer* and *Teisseyre*, 1988).

In order to get a rough impression about the resulting changes of the apparent resistivities we assume a rather simple two-dimensional model of the resistivity structure,

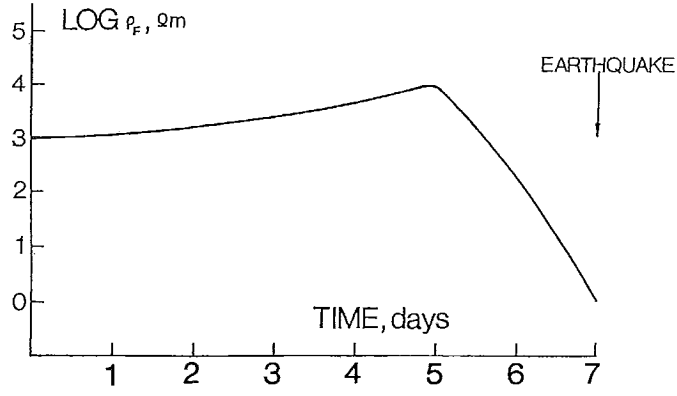

Fig. 1. Tentative model of temporal resistivity changes in the earthquake fault area prior to occurrence of the event. Rupture is marked by an arrow. Gradual increase of resistivity in the epicentral area (zone of dilatancy) is followed by a sharp decrease due to percolation of water into the system of microcracks. This is controlled by a threshold process of crack evolution (nucleation of microcracks) in the imminent stage prior to rupture.

including an elliptic-shape fault zone (Figs. 2a-7a, lower part). We calculate the apparent resistivity response for various resistivities in the fault zone, corresponding to the model in Fig. 1. Four different periods are used, i.e. 24 h, 1 h, 60 s and 1 s. For the numerical modelling we have employed the finite difference method. The procedure is presented by *Wieladek et al.* (1981). Computational results are displayed in Figs. 2a-7a (upper part). They reveal rather demonstrative apparent resistivity anomalies across the fault zone. Naturally, these resistivity anomalies are reflected into the electric field through induction.

Any time dependence of apparent resistivity ρ_A, and thus variations in the ETF, is obtained if we employ gradual changes of the resistivity in the fault zone, as assumed in Fig. 1. Resulting time variations of apparent resistivities are displayed in Figs. 2b-7b, for five different periods, i.e. 24 h, 1 h, 60 s, 10 s, and 1 s. The apparent resistivities are computed for three sites on the earth surface; just above the elliptical fault zone (site 3 in Figs. 2a-7a), site 2 at the left edge of the fault zone and site 1 about 5 km from the left edge of the fault zone. Considering the square-root of the apparent resistivity we can directly read the relative changes between the electric and the magnetic field. In our examples we find the largest changes of ρ_A at site 3 (H-polarization), in the range of up to several orders of magnitude for our particular models (see Figs. 2b-7b).

From these results we summarize some general conclusions:

1. A near-surface earthquake-preparational zone provides larger "anomalous" electromagnetic induction effects than a deeper located one (cf. Figs. 2 and 3).
2. In the presence of a superficial layer (with constant resistivity) "anomalous" induction effects increase with decreasing thickness of the layer (cf. Figs. 4 and 5).
3. Considering a superficial layer of constant thickness "anomalous" induction effects increase with increasing resisitivity in the layer (cf. Figs. 5 and 6).
4. The location of the recording site with regard to the position of the elliptical earthquake zone is of decisive importance. For our fault dimensions chosen the "anomalous" induction effects decrease rapidly with distance from the centre of the fault (elliptic body).

Our examples provide a good demonstration about the qualitative changes of apparent resistivity in the vicinity of a body where stress-induced crack development prevails. The quantitative changes of ρ_A depend of course on the model assumed. Our models are arbitrary and the results provide only an idea about possible apparent resistivity changes. The choice of the model is decisive for the magnitude of apparent resistivity changes, as well as the location of the recording site in relation to the location of the fault area (= elliptic body). The deployment of a recording station just above the fault (= site 3 in our models, the position of which is however not known a priori) provides largest apparent resistivity variations.

Meyer and *Teisseyre* (1988, 1989) have suggested the existance of stress induced anisotropy of electric conductivity. Relating the resistivity response of a tectonic stress system to the principal axes of the fault plane of an impending earthquake, we may expect sectors of dilatancy and compression. Different crack development in these sectors (geometrical orientation, opening and closing of cracks) would thus provide an anisotropy of electric conductivity. In electromagnetic interpretation we can compute polar diagrams of the electromagnetic field. The polarisation axes reflect in general the orientation of geological microstructures and/or macrostructures. On the other hand, any temporal changes of polarisation axes may be interpreted by changes in the geometrical orientation of microcracks within a system under stress, i.e. an earthquake preparational zone.

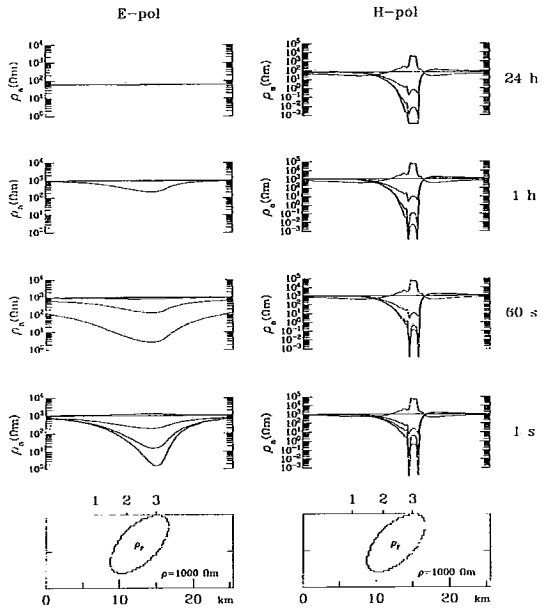

Fig. 2a. Apparent resistivity response at the Earth surface for an extremely simplified 2D resistivity structure, including an anticipated elliptic earthquake fault area. Left side: E-polarization; right side: H-polarization. The 1000 Ohm-m layer has a presumed thickness of 400 km, overlying a halfspace with a resistivity of 10 Ohm-m. Resulting apparent resistivities increase with increasing resistivity in the fault zone: lowest curves for 1 Ohm-m, uppermost curves for 10000 Ohm-m, according to the model in Fig. 1. Apparent resistivity responses are computed for four different periods: 24 hours, 1 hour, 1 minute and 1 second. The resistivity model is displayed in the bottom of the figure and responses for the different periods on top. Location of fault area: Surface fault, no sedimentary layers. The resulting apparent resistivities increase with increasing resistivity, ρ_F, in the fault zone: lowest curves for 1 Ohm-m, uppermost curves for 10000 Ohm-m.

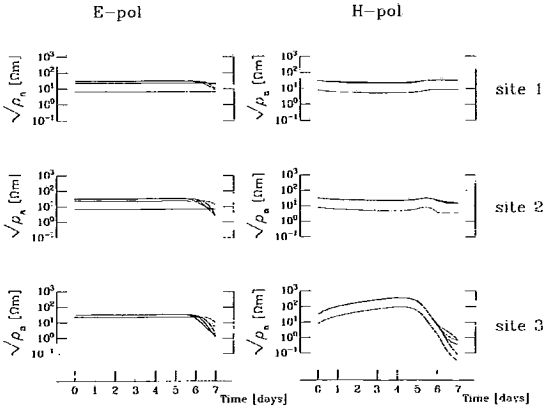

Fig. 2b. Time dependence of apparent resistivity changes (square-root), $\sqrt{\rho_A}$, using the model of temporal resistivity variations in the fault zone according to Fig. 1 and the resistivity structure model in Fig. 2a. The computations are carried out for five different periods, 24 h, 1 h, 60 s, 10 s and 1 s, at the three sites 1, 2 and 3 (see Fig. 2a). The square-root of the apparent resistivity in proportional to the ratio of electric field over magnetic field variations. For this particular case temporal changes of $\sqrt{\rho_A}$ are in the range of 3 orders of magnitude at site 3, basically independent of the periods considered (24 h to 1 s).

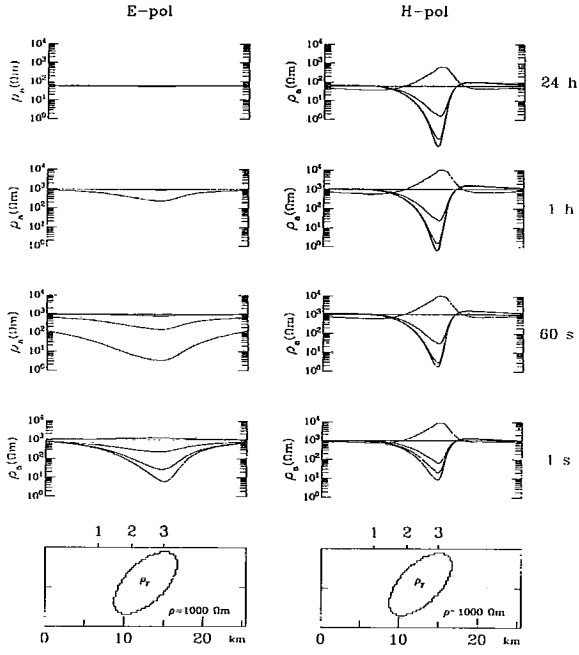

Fig. 3a. Same general assumption as in Fig. 2a. However, fault zone does not reach the surface. Distance between surface to top of the fault zone is assumed to 500 meters. Resulting apparent resistivities increase with increasing resistivity in the fault zone: lowest curves for 1 Ohm-m, uppermost curves for 10000 Ohm-m.

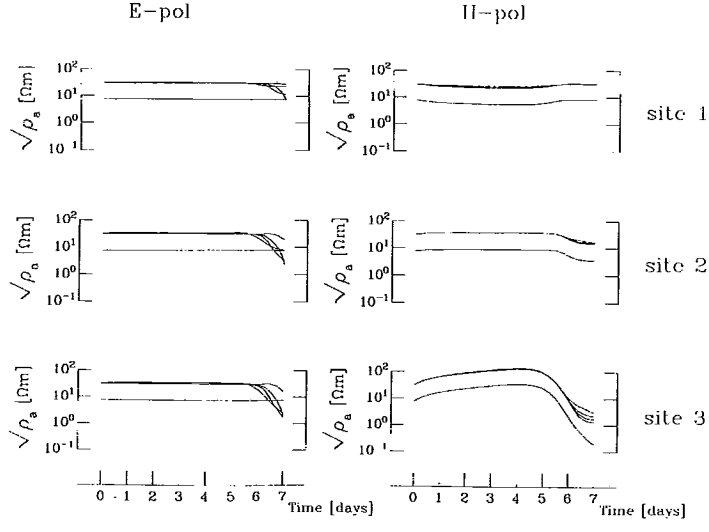

Fig. 3b. Same as in Fig. 2b, but for the resistivity structure model of Fig. 3a. For this particular case temporal changes of $\sqrt{\rho_A}$ are in the range of about 2 orders of magnitude at site 3, independent on the periods considered.

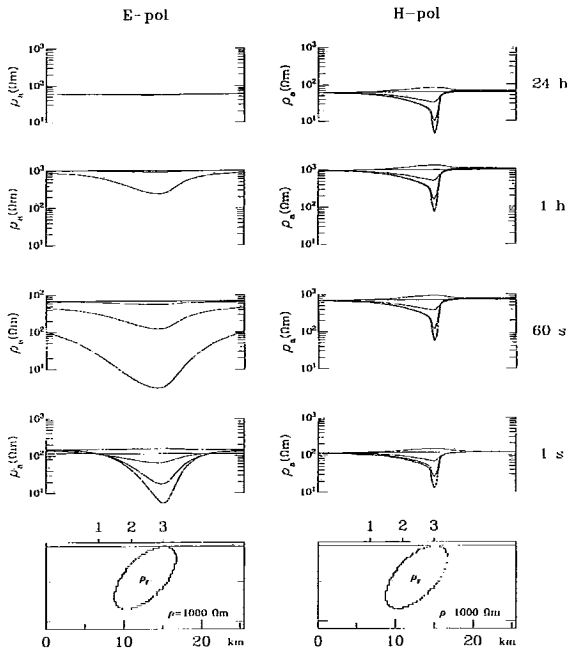

Fig. 4a. Same general assumptions as in Fig. 2a. The fault zone does not reach the surface and a superficial layer is included. Distance between surface to top of the fault zone = 500 m. Thickness of the superficial layer = 500 m, resistivity in the superficial layer = 20 Ohm-m. Resulting apparent resistivities increase with increasing resistivity in the fault zone: lowest curves for 1 Ohm-m, uppermost curves for 10000 Ohm-m.

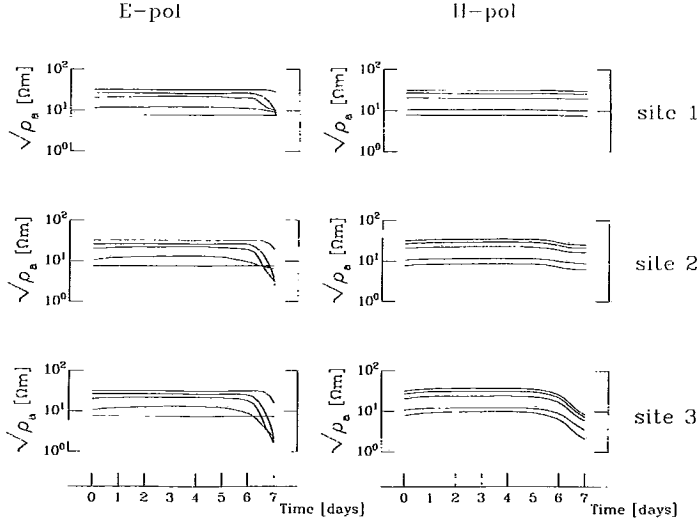

Fig. 4b. Same as in Fig. 2b, but for the resistivity structure model of Fig. 4a. The influence of the superficial layer is directly obvious, manifested in the smaller values of $\sqrt{\rho_A}$, compared with the previous models without the superficial layer.

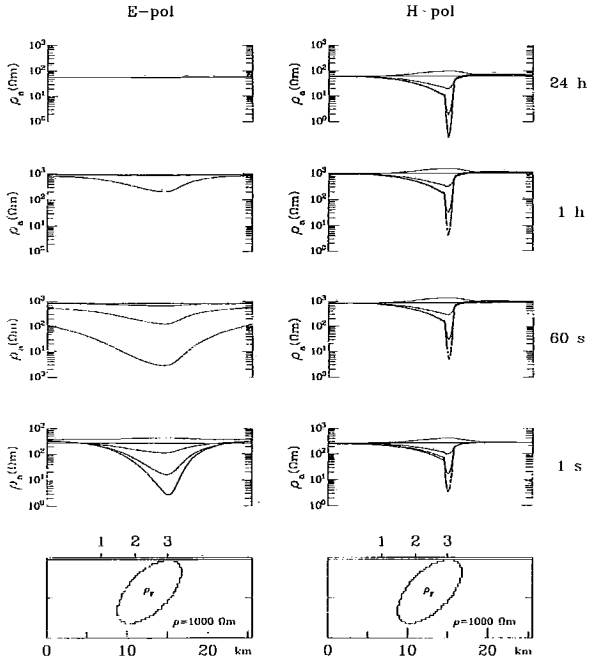

Fig. 5a. Same general assumptions as in Fig. 2a. The fault zone does not reach the surface and a superficial layer is included. Distance between surface to top of the fault zone = 250 m. Thickness of the superficial layer = 250 m, resistivity 20 Ohm-m. Resulting apparent resistivities increase with increasing resistivity in the fault zone: lowest curves for 1 Ohm-m, uppermost curves for 10000 Ohm-m.

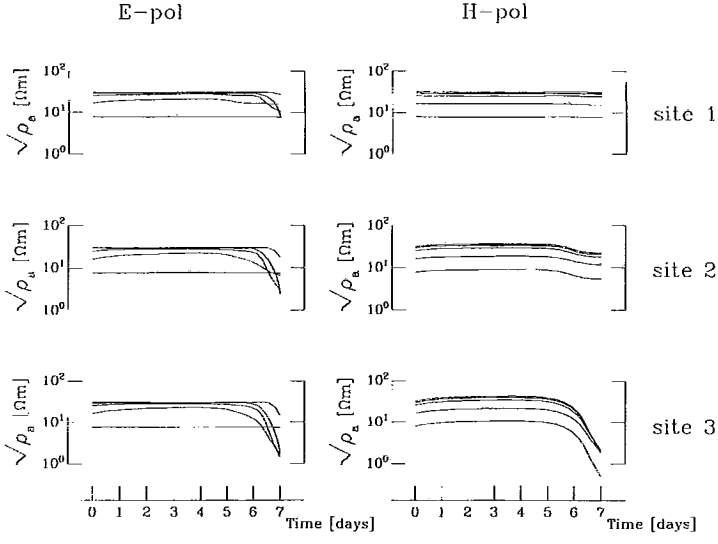

Fig. 5b. Same as in Fig. 2b, but for the resistivity model of Fig. 5a. The lesser thickness of the superficial layer (compared to the model in Fig. 4a) provides slightly larger values of $\sqrt{\rho_A}$.

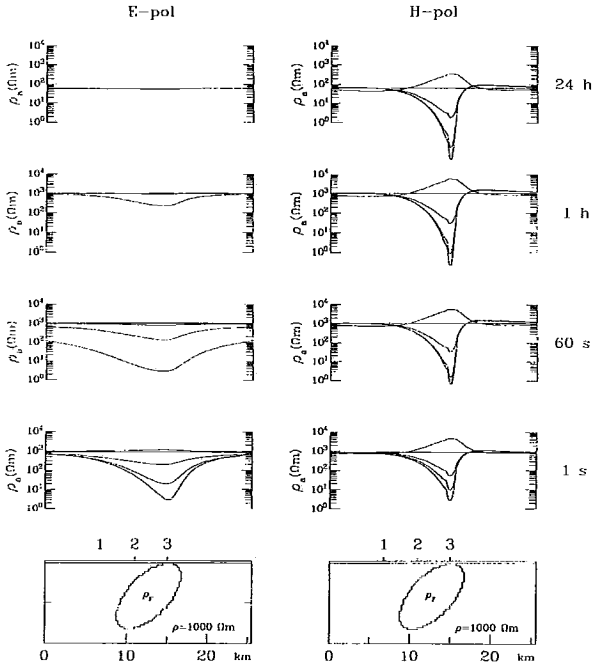

Fig. 6a. Same general assumptions as in Fig. 2a. The fault does not reach the surface and a superficial layer is included. Distance between surface to top of the fault zone = 250 m. Thickness of the superficial layer= 250 m, resistivity 200 Ohm-m. Resulting apparent resistivities increase with increasing resistivity in the fault zone: lowest curves for 1 Ohm-m, uppermost curves for 10000 Ohm-m.

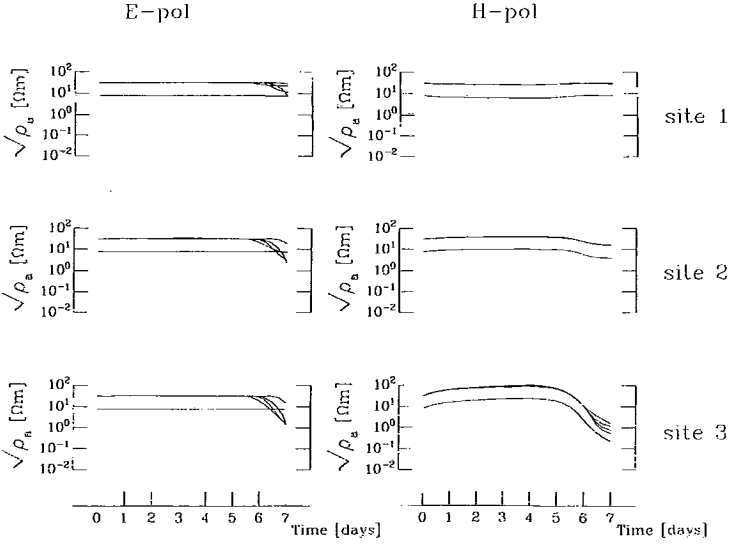

Fig. 6b. Same as in Fig 2b, but for the resistivity model in Fig 6a. Increasing the resistivity in the superficial layer from 20 to 200 Ohm-m we obtain larger values of $\sqrt{\rho_A}$, compared to the model in Fig. 5a.

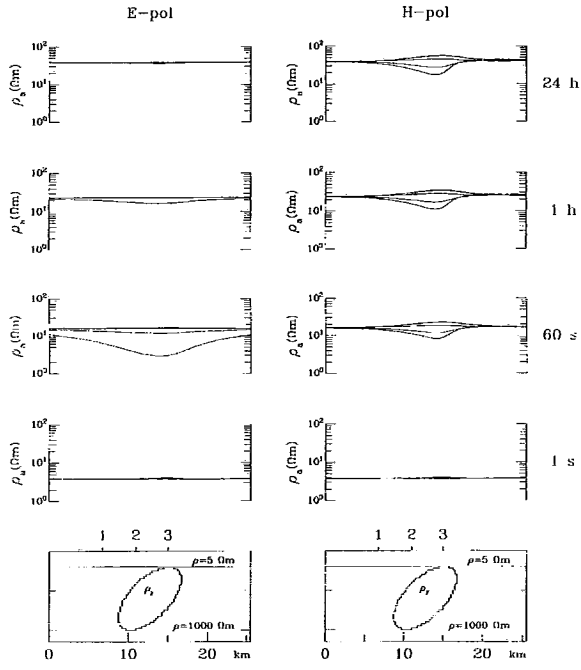

Fig. 7a. Same general assumptions as in Fig. 2a. The model used here refers to a more realistic resistivity structure at Wendo Genet, a site in the Main Ethiopian Rift. It is obtained from a preliminary analysis of MT-data from this area. The model includes a low resistivity superficial sedimentary layer (thickness = 2 km, ρ = 5 Ohm-m). Different curves demonstrate apparent resistivities using 1, 10, 100, 1000 and 10000

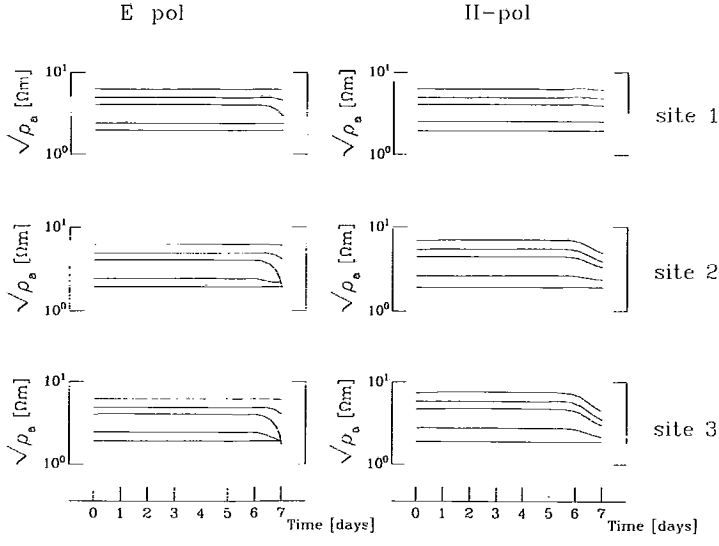

Fig. 7b. Same as in Fig. 2b, but for the model in Fig. 7a. The low resistivity superficial layer provides smaller temporal changes of $\sqrt{\rho_A}$, numerical values of which are about 3 at site 3.

3. *Apparent resistivity changes and seismic energy release*

Any time dependence of apparent resistivities may be related to stress conditions and processes at different stages prior, during and after the occurrence of the seismic event (for instance: stress accumulation, crack orientation and crack density, percolation processes, stress release). One measurable process is the stress release by earthquakes. Seismic energy is related to earthquake magnitude through the relation (*Båth*, 1979)

$$log\ E = a + bM \tag{4}$$

where E is seismic energy in ergs, M is the earthquake magnitude and a,b are constants. We can estimate the amount of seismic energy released per unit time and relate these measures to the time variation of apparent resistivities. Thus, we generate two time series, describing the time variations of the apparent resistivity and seismic energy release. Any correlation of the two time series will prove a causal relationship between tectonic stress (earthquake energy release) and crack development (resistivity changes) during an earthquake cycle. Especially information about the preseismic phase may provide valuable news for earthquake forecast.

Correlation of the two time series can be achieved through visual inspection. Else, a more objective method of crosscorrelation may be preferred. The crosscorelation function of two time series is a function of the mutual time shift τ. This function is commonly normalized, having values in the range 1 (perfect coherence) and -1 (perfect coherence, but opposite phase). The normalized crosscorrelation function is defined as:

$$\gamma(\tau) = \frac{1}{(N-\tau)\sqrt{\delta_x\,\delta_y}} \sum_{i=1}^{N-1} X_i\, Y_{i+\tau} \tag{5}$$

X_i, Y_i are samples of the time series and δ_x, δ_y are the corresponding amplitude variances.

4. *ETF residual analysis*

Using estimated transfer functions we can predict the electric field from magnetic observations. The residual of the ETF is obtained as the difference of the predicted and the observed electric field. The investigation of the residual can easily reveal variations which have a different nature than those connected with electromagnetic induction. Streaming potentials or electrokinetic effects, related to dilatancy prior to earthquakes, have, for instance, been proposed by *Mizutani et al.* (1976), *Murakami et al.* (1984) or *Miyakoshi* (1986). *Varotsos* and *Alexopoulos* (1986, chapt. 7) ascribe certain ETF anomalies to a stress induced source effect, related to physical properties of rocks under stress. Heterovalent impurities in ionic crystals cause interstitials which form electric dipoles. By changing the imposed stress field, the dipoles re-orientate into a new state of

thermodynamic equilibrium, the time process of which may be fast under certain stress conditions. The resulting change of polarization is equivalent to the emission of an electric current. After a thorough removal on possible sources of electric noise, the interpretation of the remaining residual may show anomalies which are connected with the generation of electric currents, such as those caused by crack development, creep motion or emission of electric currents described by *Varotsos* and *Alexopoulos*, 1986 (re-orientation of dipoles in ionic crystals).

5. *Conclusions*

1. The tentative model chosen in this work reveals significant resistivity changes prior to earthquakes. A continuous search in the ETF may thus provide indications for forthcoming earthquakes.

2. From the results of this particular model it is quite obvious that the anomalous resistivity changes are concentrated to regional limited sites (in our case site 3). However, these optimal sites are not apriori known and a "mislocation" of a recording site may not give any anomalies at all. This is clear from the site responses at site 1 and site 3, only 10 km separated from each other. Using other models we may get quite different results. For instance, the Extended Dilatancy Anisotropy model (EDA), proposed by *Crampin et al.* (1984), suggests crack evolution over large areas, much larger than the limited area used in our model.

Acknowledgements

This research is conducted jointly by the Seismological Department, University of Uppsala and the Institute of Geophysics, Polish Academy of Science, Warsaw. We are grateful to Prof. J. Jankowski and Prof. R. Teisseyre for fruitful discussions. The Swedish Academy of Science and the Polish Academy of Sciences provided appreciated support through their exchange program. Financial support was also provided through the Committee of Scientific Investigations (KBN) of Poland, grant nr. 607389101.

References

Barsukov, O.M., 1972: Variations of electric resistivity of mountain rocks connected with tectonic causes. In: E.F. Savarensky and T. Rikitake (Editors). Forerunners of Strong Earthquakes. *Tectonophysics*, **14**(3/4): 273-277.

Barsukov, O.M. and O.N. Sorokin, 1973: Variations in apparent resistivity of rocks in the seismically active Garm region. *Izv., Earth Physics*, **10**, 100-102.

Bernard, P., 1992. Plausibility of long distance electrotelluric precursors to earthquakes. *J. G. R.*, **97**, B12, 17531-17546.

Båth, M., 1979: Introduction to Seismology. Birkhäuser, 2nd ed., 428 pp.

Crampin, S., R. Evans and B.K. Atkinson, 1984: Earthquake prediction: a new physical basis. Proceedings of the First International Workshop on Seismic Anisotropy, Suzdal, 1982, ed. Crampin, S., Hipkin, R.G., and Chesnokov, E.M., *Geophys. J.R. Astr. Soc.*, **76**, 147-156.

Ernst, T., J. Marianiuk, C.P. Rozluski, J. Jankowski, A. Palka and R. Teisseyre, 1991: Analysis of the magneto-telluric recordings from the Friuli seismic zone, NE Italy. *Acta Geophys. Pol.*, **34**, 2, 129-158.

Mazzella, A. and H.F. Morrison, 1974: Electrical resistivity variations associated with earthquakes on the San Andreas fault. *Science*, **185**, 855-857.

Meyer, K., and R. Teisseyre, 1988: Electrotelluric periodic anomalies prior to large imminent earthquakes. Presented at the IASPEI assembly 1985, Tokyo. *Acta Geophys. Pol.*, **36**, 4, 309-322.

Meyer, K. and R. Teisseyre, 1989: Observation and qualitative modelling of some electrotelluric earthquake precursors. Presented at the IASPEI assembly, Vancouver 1987. *Phys. Earth Plan. Int.*, **57**, 45-46.

Miyakoshi, J., 1986: Anomalous time variation of the self-potential in the fractured zone of an active fault preceding the earthquake occurrence. *J. Geomagn. Geoelectr.*, **38**, 1015-1030.

Mizutani, H., T. Ishido, T. Yokokura and S. Ohnishi., 1976: Electrokinetic phenomena associated with earthquakes. *Geophys. Res. Lett.*, **3**, 365-368.

Murakami, H., H. Mizutani and S. Nabetani, 1984: Self-potential anomalies associated with an active fault. *J. Geomagn. Geoelectr.*, **36**, 351-376.

Niblett, E.R. and Y. Honkura, 1978: Time dependence of electromagnetic transfer functions and their association with tectonic activity. 4th Workshop on Electromagnetic Induction, Murnau, FRG, 17 pp.

Stopinski, W. R. and Teisseyre, 1982: Precursory rock resistivity variations related to mining tremors. *Acta Geophys. Pol.*, **30**(4).

Teisseyre, R., 1983: Premonotory mechanism and resistivity variations related to earthquakes. *Pure Appl. Geophys.*, **121**(2), 297-315.

Teisseyre, K., 1991: Simulation of anisotropic changes of resistivity in primarily anisotropic rocks under load. *Acta Geophys. Pol.*, **34**, 3, 315-334.

Wieladek, R., K. Nowozynski and Z. Tarlowski, 1981: Application of the Cholesky-Banachiewicz Method to solving some linear systems of equations approximating Helmholtzs equation. Publ. Inst. Geophys. Pol. Acad. Sc., G-2, 143, 3-12.

Varotsos, P. and K. Alexopoulos, 1986: Thermodynamics of point defects and their relation with bulk properties. North-Holland Phys. Publ., 474 pp.

Zadro, M., T. Ernst, J. Jankowsk, C.P. Rozluski and R. Teisseyre, 1990: Magneto-telluric recordings from the Friuli seismic zone, northeast Italy. *Tectonophysics*, **180**, 303-308.